International Journal of Fluid Power, 2015
Vol. 16, No. 3, 179–187, http://dx.doi.org/10.1080/14399776.2015.1110094

Taylor & Francis
Taylor & Francis Group

Modelling of the influence of entrained and dissolved air on the performance of an oil-hydraulic capacity

Katharina Schmitz* and Hubertus Murrenhoff

Institute for Fluid Power Drives and Controls, RWTH Aachen University, Steinbachstr. 53, 52074 Aachen, Germany

(*Received 7 August 2015; accepted 15 October 2015*)

Fluids used in fluid power systems to transmit power and energy seldom consist of pure oil due to a large number of impurity sources. Especially impurities in form of air bubbles highly change the system behaviour with respect to stiffness and efficiency. The aim of this paper is to provide a mathematical model to simulate the effect of air on the pressure build-up and release in an oil-hydraulic capacity. Therefore, first a model to calculate the mass transfer between dissolved and entrained air is presented. In the end, the new developed model is validated with measurements.

Keywords: entrained air; dissolved air; air mass transfer; lumped parameter simulation; bulk modulus

1. Introduction

The fluid in most hydraulic applications cannot be assumed to only consist of pure hydraulic oil. Before oil is filled into a hydraulic system it has been in contact with air during production and transportation so that air molecules always exist in hydraulic pressure fluids. This air usually is invisible; it is dissolved in the oil due to the capability of oil to solve a certain amount of air. This solvable quantity depends on the pressure and on the kind of fluid. Dissolved air does not negatively affect the properties of oil (Ivantysyn and Ivantysynova 2001) and can therefore not be measured.

When the pressure falls below the equilibrium pressure dissolved air can be released from the oil and visible air bubbles form, see also Zhou et al. (2013) for detailed information. In addition entrained air can enter a system if the reservoir is designed badly when the fluid flows through air as a free jet and air bubbles are carried inside the fluid or when the pump sucks air caused by a leaking low pressure line. Entrained air leads to changes in fluid properties, results in a higher chance of cavitation which damages system components and leads to higher losses in system components (Ivantysyn and Ivantysynova 2001, Murrenhoff 2014). Air also reduces fluids bulk modulus and therefore changes system behaviour and stiffness severely.

System simulation tools in form of lumped parameter models are commonly used in fluid power to design and optimize hydraulic systems. Most simulation tools do not consider impurities like air bubbles and therewith changed fluid properties or they provide only rough models with several restrictions. The calculation of the pressure build-up is the key factor in fluid power simulations. Standardly, simulation programs have a modular design consisting of nodes or pressure generator components which link different hydraulic components. The pressure is calculated inside these nodes based on information about the volume respectively mass flow and the volume change of the attached components (Esqué and Ellman 2005, Riedel *et al.* 2010, von Grabe *et al.* 2014).

Previous measurements with the test-rig displayed in chapter 4 have shown that the pressure change in a sealed volume variable capacity highly depends on the entrained air content (Schrank 2015), see Figure 1.

In this figure the pressure is illustrated over the relative volume change of this sealed volume for two different amounts of entrained air. With increasing amount of air the pressure needs more volume change to increase due to a reduced stiffness and a reduced bulk modulus. This behaviour has often been observed and is described for example in (Kim, 2012).

In contrast to literature, in the measurements shown in Figure 1 not only the pressure build-up but also the pressure release is shown. Especially in the curve with a large amount of entrained air a hysteresis can be detected; the curves of the pressure build-up and pressure release are not congruent. This can be explained by the pressure depended changing of air dissolve capacity of the oil and has been observed also by e.g. (Zhou *et al.* 2013) and (Manhartsgruber 2013). Because of its deep impact on system behaviour this phenomenon should be investigated and mass transfer between entrained and dissolved air has to be modeled to be able to simulate the pressure change in a two-phase capacity.

2. Existing model to describe the pressure build-up and decrease

The calculation of the pressure is important for all hydraulic systems simulation tools. The commonly used

*Corresponding author. Email: post@ifas.rwth-aachen.de

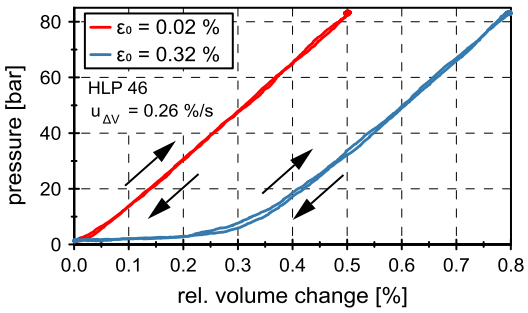

Figure 1. Pressure change in a sealed volume variable capacity.

equation to calculate the pressure change in a liquid filled capacity is shown in Equation (1). Here, the pressure change is proportional to the relative change in mass inside the capacity and to the relative change in volume. The bulk modulus E is defined to be the proportional factor in this equation (Murrenhoff 2014)

$$dp = E\left(\frac{dm}{m} - \frac{dV}{V}\right) \tag{1}$$

Depending on the fluid, the bulk modulus of oil is not a constant value but depends on the pressure. A simple model to take the pressure dependent variation into account is Equation (2). E_0 is the bulk modulus of the oil at atmospheric pressure p_0 and M is a fluid dependent pressure factor, which has to be experimentally determined. For most standard mineral oils the pressure factor is equal 10.

$$E_l = E_0 + M(p - p_0) \tag{2}$$

The effects of entrained air inside the liquid filled capacity can be estimated by using an effective bulk modulus in Equation (1). Different models exist for its calculation. Many of them are described in (Gholizadeh *et al.* 2012) and selected ones are discussed below. In general, these models can be distinguished between models that do not take a mass transfer into account and in models that include mass transfer effects of entrained and dissolved air.

2.1. Model excluding mass transfer

A commonly used model to calculate the effective bulk modulus is Equation (3). It is based on the volume balance on a capacity filled with an oil and an air phase. The stiffness of the oil phase is assumed to be calculable with Equation (2) and the air phase is modelled with the ideal gas law. The derivation of Equation (3) can be found in (Murrenhoff 2014). In this equation ε_0 is the void fraction of air at atmospheric pressure and n is the polytrophic exponent which depends on the state of process. For an isothermal process n is equal to 1, for an ideal isotropic process it is equal to 1.4 for air.

$$E_{\mathrm{Mur}} = \frac{(1-\varepsilon_0)\left(1+\frac{M(p-p_0)}{E_0}\right)^{-\frac{1}{M}} + \varepsilon_0\left(\frac{p_0}{p}\right)^{\frac{1}{n}}}{\frac{(1-\varepsilon_0)}{E_0}\left(1+\frac{M(p-p_0)}{E_0}\right)^{-\frac{M+1}{M}} + \frac{\varepsilon_0}{np_0}\left(\frac{p_0}{p}\right)^{\frac{n+1}{n}}} \tag{3}$$

This model has been successfully validated with measurements in Kim (2012) but has the restriction that no mass transfer between dissolved and entrained air can be taken into account.

2.2. Models including mass transfer

Different models exist that take a mass transfer into account. The most commonly used one is the Henry-Law that characterizes the equilibrium of solvable gas in a liquid, Equation (4). The ratio θ between the void fraction of entrained gas $\varepsilon_{g,e}$ and the fraction of gas existing in liquid or gaseous state inside the system is linearly dependent on the static pressure p and the saturation pressure p_{sat}.

$$\frac{\varepsilon_{g,e}(p)}{\varepsilon_g} = \theta_{\mathrm{Henry}}(p) = 1 - \frac{p - p_{\mathrm{vap}}}{p_{\mathrm{sat}} - p_{\mathrm{vap}}} = 1 - y \tag{4}$$

At pressures higher than the saturation pressure all gas is dissolved inside the oil and θ is equal to 0. At pressures between the saturation pressure and the vapour pressure p_{vap} air bubbles are present inside the oil and a two-phase fluid forms $0 < \theta < 1$. The saturation pressure is dependent on the amount of gas inside the system and also on the fluid dependent Henry constant.

To use the Henry-Law in simulation programs, modifications must be made to avoid the discontinuity at saturation pressure and vapour pressure, e.g. see Equation (5) from the program Amesim by LMS (2009). A similar model was also developed and used by Vacca *et al.* (2010).

$$\theta_{\mathrm{LMS}}(p) = (1-y)^5\left(1 + 5y + 15y^2 + 35y^3 + 70y^4\right) \tag{5}$$

In experimental investigations, Gholizadeh determined that entrained air cannot be completely dissolved inside the oil at normal time durations even if the saturation pressure is highly exceeded. Therefore he developed a new model to describe the ratio between undissolved gas and total amount of gas inside the system (Gholizadeh 2013), Equation (6).

$$\theta_{\mathrm{Gho}}(p) = \left(\frac{p_c - p}{p_c - p_{\mathrm{vap}}}\right)(1 - \theta_c) + \theta_c \tag{6}$$

He introduced a critical pressure pc that is higher than the saturation pressure and marks the pressure above which no more entrained air can be dissolved inside the liquid. The ratio between entrained air and total air inside the system above the critical pressure is θ_c. In addition, the critical pressure is depended on the change of state. For a slow and isothermal pressure rise the critical pressure is lower than the saturation pressure. In contrast, for a fast and adiabatic pressure rise the critical pressure

shifts to higher pressures and more entrained air cannot be dissolved inside the oil at higher pressures.

A summary of the discussed models can be found in Figure 2. Here the ratio between entrained air to total amount of air inside the system is plotted over the pressure. At vapor pressure no air can be dissolved inside the liquid and therefore the ratio is equal to 1. These static models only allow the calculation of the equilibrium state but do not account for the time needed to reach this equilibrium. The model of Gholizadeh makes an approach to take the time depended factor into account by the variation of the critical pressure.

The different models to calculate the amount of dissolved and entrained air lead to different pressure dependent values of the bulk modulus. The equations proposed to calculate the bulk modulus of LMS (Equation (7)) and Gholizdeh (Equation (8)) are in analogy to the equation used by Murrenhoff (Equation (3)) but allow the consideration of temperatures other than norm temperature and also the variable, pressure dependent change in entrained air.

$$E_{\mathrm{LMS}} = \frac{(1-\varepsilon_0)\left(1+\frac{M(p-p_0)}{E_0}\right)^{-\frac{1}{M}} + \varepsilon_0\theta_{\mathrm{LMS}}\frac{T}{T_0}\left(\frac{p_0}{p}\right)^{\frac{1}{n}}}{\frac{(1-\varepsilon_0)}{E_0+M(p-p_0)}\left(1+\frac{M(p-p_0)}{E_0}\right)^{-\frac{1}{M}} + \frac{\varepsilon_0\theta_{\mathrm{LMS}}}{np}\frac{T}{T_0}\left(\frac{p_0}{p}\right)^{\frac{1}{n}}} \quad (7)$$

For the model used by Gholizadeh, the bulk modulus is calculated independently for the two sections, at pressures between the vapour pressure and the critical pressure and at pressures above the critical pressure. Above the critical pressure the bulk modulus is equal to values calculated with models that exclude phase change. In addition, the change of state of the gas n_i can be selected independently for both sections.

$$E_{\mathrm{Gho}} = \frac{(1-\varepsilon_0)\left(1+\frac{M(p-p_0)}{E_0}\right)^{-\frac{1}{M}} + \varepsilon_0\theta_{\mathrm{Gho}}\frac{T}{T_0}\left(\frac{p_0}{p}\right)^{\frac{1}{n_i}}}{\frac{(1-\varepsilon_0)}{E_0+M(p-p_0)}\left(1+\frac{M(p-p_0)}{E_0}\right)^{-\frac{1}{M}} + \frac{\varepsilon_0\theta_{\mathrm{Gho}}}{n_i p}\frac{T}{T_0}\left(\frac{p_0}{p}\right)^{\frac{1}{n_i}}} \quad (8)$$

A summary of the discussed equations to calculate the bulk modulus can be found in Figure 3. The pressure dependent bulk modulus is shown for an oil-air mixture with the indicated parameters and an initial void fraction of 2% at atmospheric pressure.

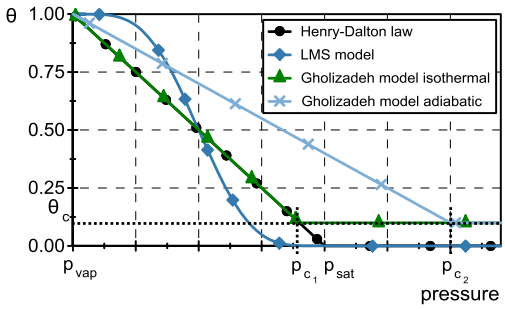

Figure 2. Pressure dependent calculation models of the dissolved air content.

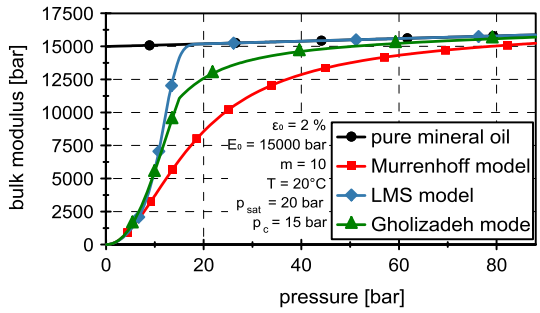

Figure 3. Different pressure dependent bulk-modulus models.

The linearly increasing bulk modulus of pure mineral oil shows the upper limit for all models. The model of Murrenhoff which does not include any phase change depicts the lower limit of all bulk modulus curves as it only describes the pressurization of the air bubbles and their pressure dependent volume shrinkage. The models that calculate a pressure dependent phase change lie in between these curves. For the LMS model all air is dissolved at pressures above the set saturation pressure of 20 bar and the bulk modulus is equal to the one of pure mineral oil. In contrast, with the Gholizadeh model air is dissolved up to a critical pressure set to 15 bar and after the bulk modulus follows the curve of an oil-air mixture with a lower but constant air content.

In addition to the models with a pressure dependent mass transfer, new models with time constants have recently been developed. One example is the model presented by Zhou et al. (2013) which describes the transfer between dissolved and entrained air in dependency of the time. This model is based on the Full Cavitation Model by Singhal developed for the use in computational fluid dynamic simulations. Basis is the assumption that the Reyleight–Plesset equation to describe the dynamic of gas bubbles is also valid for air bubbles. When the mass fraction of entrained air $\mu_{g,e}$ is lower than the equilibrium mass fraction $\mu_{g,eq}$ according to Henry-Law, then air bubbles for and the time dependent change in mass fraction of entrained air is positive. Otherwise entrained air is being dissolved and the rate is negative, see Equation (9).

$$\frac{d\mu_{g,e,\mathrm{Zhou}}}{dt} = \begin{cases} \frac{k_1}{\tau}\left(\mu_{g,eq}-\mu_{g,e}\right)\sqrt{|p_{eq}-p|} & \mu_{g,e} \le \mu_{g,eq} \\ -\frac{k_2}{\tau}\mu_{g,e}\sqrt{|p-p_{eq}|} & \mu_{g,e} > \mu_{g,eq} \end{cases} \quad (9)$$

The driving force of the absorption process is the existing fraction of dissolved air inside the oil, which is the difference between equilibrium fraction of entrained air and existing entrained air at each time step. The velocity of the absorption and desorption process is considered in this model by the use of two constants k_1 and k_2 and a characteristic time of the system τ. The two constants must be determined experimentally.

3. New model to predict the mass transfer between entrained air and dissolved air

All models presented above use the simplification of only consider the static pressure for the calculation of the transfer between entrained and dissolved air. To be able to increase the accuracy of the calculations a more precise model is presented here.

3.1. *Experimental investigation of the mass-transfer*

To be able to model the mass transfer, the influencing parameters must be known. Therefore measurements are performed on a test-rig, set-up at the Institute of Fluid Power Drives and Controls in Aachen, Germany. The schematic layout of this test-rig can be found in Figure 4.

It consists of a sealed measurement chamber with a volume variable from 6.23 to 6.29 L. The variation in volume is performed by a cylinder that is controlled by a servo valve (V4 in the figure). Therewith a volume change of about 1% with a constant volume change rate is possible. Due to the change in volume, the pressure inside the chamber can be varied between 0.1 and 80 bars absolute. The walls of the measuring chamber that contains the test fluid have a minimal width of 40 mm to minimize volume changes due to the expansion of the measuring chamber caused by raising pressures.

The absolute pressure inside the measuring chamber is logged by a Hydac HDA 3800 pressure sensor with a range of 0–100 bars. In addition this sensor can be exchanged to a Suchy SD-33 pressure sensor with a range of 0–2.5 bars to allow the precise measurement below atmospheric pressure. The volume change of the chamber is logged by a potentiometric Burster 8711-100 position sensor with a range of 0–100 mm located at the piston outside the test chamber. A Hydac ETS 4000 temperature sensor provides information about the temperature of the fluid inside the measuring chamber. Measurements are executed by filling the chamber with oil that has not been used before and that has been stored several months at atmospheric pressure. Therefore it is guaranteed that the oil is completely saturated with dissolved air at atmospheric pressure. Almost all free air

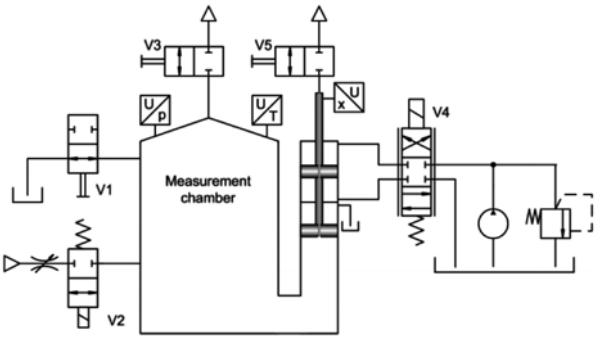

Figure 4. Set-up of the test-rig.

is removed from the test chamber for the start of the measurements.

Two different measurements are possible with the test-rig, see Figure 5. On the left side of the figure measurements start with a large fluid volume and the volume is reduced by the movement of the cylinder. Therefore the pressure rises from atmospheric up to about 80 bars and the pressure build-up and decrease can be investigated. In contrast, on the right side a measurement curve is shown that starts at a low chamber volume. By increasing the volume the pressure reduces from atmospheric pressure down to about 0.1 bars absolute. Due to an equilibrium between dissolved and entrained air at atmospheric pressure, the pressure depended air release behaviour of the oil can be studied. The volume change velocity is controlled in both types of measurements and is constant for the volume increase and decrease. Between the volume increase and decrease a pausing time of 10 s is included.

It is not possible to remove all free air before the measurements and therefore the initial air content is determined by using the measurement curves of the pressure rise vs. volume decrease as discussed in (Ruan and Burton 2006). For the measurements above atmospheric pressure different initial amounts of entrained air can be included into the fluid by using pressurized air. A detailed description of the filling and measurement execution procedure can be found in Schrank *et al.* (2013). The measurements below atmospheric pressure are performed with a minimal amount

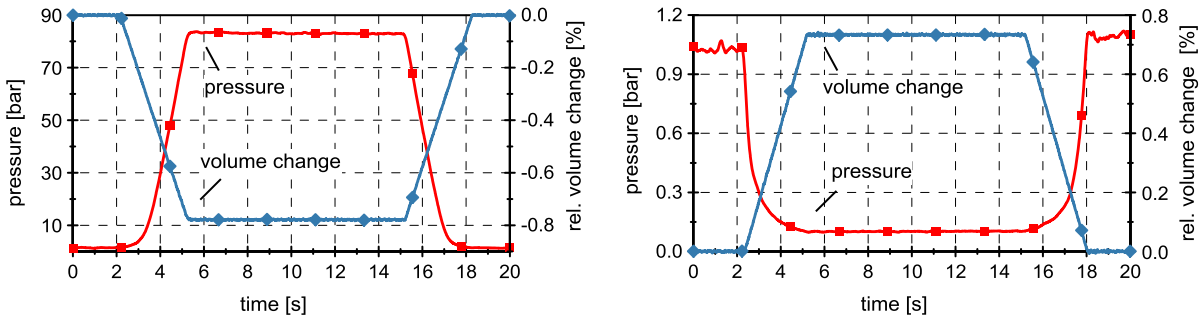

Figure 5. Exemplary measurement curves.

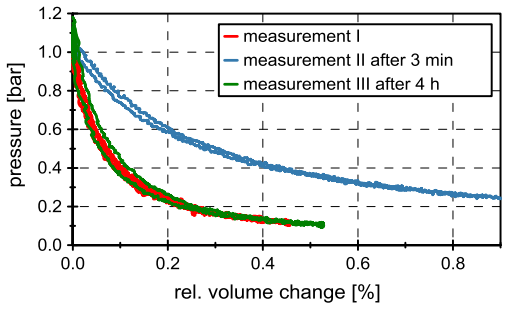

Figure 6. Measurements of the reproducibility.

of free air inside the fluid. To allow knowledge of the initial conditions inside the chamber one measurement above atmospheric pressure is performed beforehand and the void fraction is calculated, see Ruan and Burton (2006).

For the measurements above atmospheric pressure no influence on the measurements caused by previous measurements is found. In contrast, the tests below atmospheric pressure are highly influenced by the previous measurements. Figure 6 shows three measurements below atmospheric pressure, pressure plotted over relative volume change. By increasing the chamber volume the pressure reduces and air is released from the liquid. Due to the time dependent diffusion process with different speeds for the air released and re-dissolving more entrained air exists after one measurement inside the chamber. By repeating the measurements after three minutes the same starting conditions cannot be reached and the measured curve differs from the first one. It was found that after about 4 h waiting time the conditions inside the chamber reaches the previous initial conditions. Therefore minimal pausing times of 4 h are adhered between two measurements.

All measurements below atmospheric pressure show the air release dependent hysteresis in the curves of pressure plotted over chamber volume or volume change, see also Figure 7.

Here, measurements with the mineral oil HLP46 are shown. The left diagram shows the hysteresis in the curves of the pressure plotted over the relative volume change discussed below. Due to the knowledge of the initial composition of the fluid inside the chamber and the pressure and temperature dependent density of mineral oil and air, the change in amount of entrained air can be calculated over the measurements out of data for pressure and volume. This content of entrained air is depicted over time in the right diagram in Figure 7. In this measurement, the pausing time at low pressure was set to 30 min to allow better visibility. It can be found that in the beginning of the measurements the initial entrained air mass content is about 0.6×10^{-4}% which means a mass of air of about 3 mg or a void fraction of 0.04 % inside the oil filled chamber. During expansion the entrained air mass content rises up to 1.8×10^{-4}% which is equal to a mass of 9.7 mg entrained air. In the following period of 30 min at a pressure of lower than 0.11 bar absolute the mass of air rises up to 11.2 mg (2.1×10^{-4}%). According to Henrys Law with a Henry constant of 0.08 an air mass of 598 mg is dissolved inside the liquid at atmospheric pressure when assuming that it is saturated at this pressure. At a pressure of 0.1 bar a mass of only 59.8 mg can be dissolved inside the fluid according to Henrys Law. As the fluid inside the measurement chamber is saturated with air at atmospheric pressure meaning that during the expansion and pressure drop more than 500 mg of air must be released from the oil to fulfill the equilibrium condition. This is not in correspondence to measurement results. This is caused by the strong time dependence of the desorption process as it is driven by diffusion. In addition, it is interesting to see that a larger amount of air is released during the time the pressure changes but only a slight increase is seen during the following period at a low pressure level. Therefore a new model is needed that can be used to predict the time and velocity dependent behaviour.

3.2. *Mathematical modelling and validation*

The measurements show that the amount of air that is released depends on the one hand on the static pressure and on the other hand on the velocity of the pressure change. Additional measurements showing this behaviour can be found in Schrank *et al.* (2013). The driving potential for the air to be released is given by the Henry Law and depends on the static pressure. In other models the velocity of the pressure change has never been taken

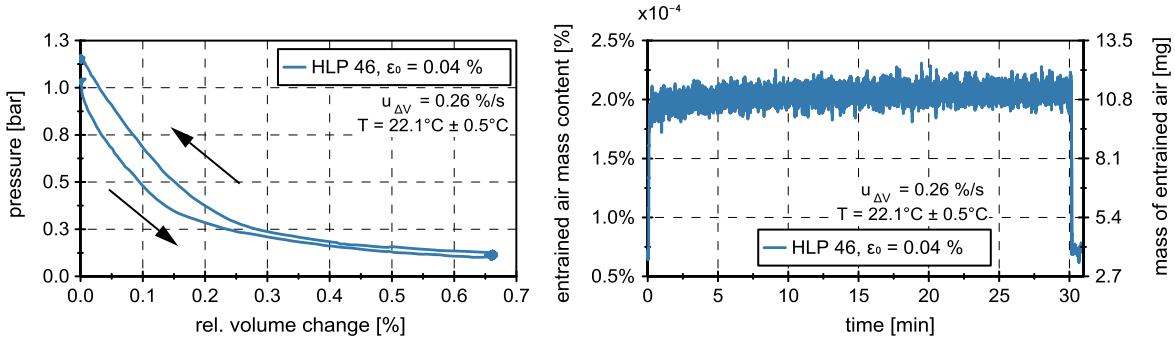

Figure 7. Pressure influence on mass-transfer.

into account. Due to the two different factors for the air release the new model consists of two independent parts, see Equation (10).

$$d\mu_{MT} = k_1 dp + k_2\left(m_{g,d,0} + m_{g,e,0} - m_{g,e} - m_{g,d,eq}\right) \quad (10)$$

The mass transfer of air that is released or dissolved is described with the two parameters k_1 and k_2 that have to be determined experimentally and rate the two summands. The second summand represents driving concentration potential which is the deviation from the equilibrium. This is described as the difference between the initial total mass of gas in dissolved and entrained state $m_{g,d,0} + m_{g,e,0}$ and the actual mass of entrained air $m_{g,e}$ and the maximal solvable amount of air at actual pressure $m_{g,d,eq}$. This amount is calculated with Henrys Law. When the sum of initial existing air is larger than the sum of actual entrained air and the maximum dissolvable air at actual pressure, then the difference in concentration balances and entrained air is dissolved inside the liquid. The time dependency of this process is given with the constant k_2. Depending on the direction of pressure change, the parameter k_2 has two alternating values as the solution process occurs much slower than the release of air.

The parameter k_1 that weights the pressure dependent summand has also two values for the absorption k_{11} and the release k_{12} of air. In addition, the factor k_{12} must be limited with the equilibrium condition. Otherwise air would be released even at pressures much higher than saturation pressure.

Figure 8 shows the comparison between the experimental results and the simulations obtained with the proposed model. In the left diagram, the relative volume change of the measurement chamber is plotted over time. This measured volume change is basis of the simulation as well as the initial conditions of the fluid inside the measuring chamber. The curves of the measured and simulated pressure are in good agreement. On the right side, the entrained air content inside the volume is shown over chamber pressure. In contrast to the measurements, the simulated course is much smoother but is also in good agreement. The used parameters for k_1 and k_2 can be found in the diagram. By comparing the curves it can be seen that the model is not able to depict all measured aspects but allows reasonable accuracy with a maximum root mean squared error of less than 8%.

4. New model to calculate the pressure change in a two phase capacity

To calculate the change in pressure of an open and volume variable system, it is expedient first to consider the volume change of the fluid. Here, the fluid consists of oil with dissolved air inside and free air. Therefore it can be described as a two phase fluid with a continuous phase (oil and dissolved air) and a dispersed phase (entrained air). The volume change of the fluid can be described independently for the different phases. By assuming the applicability of the homogeneous mixture model, meaning the neglect of mutual influences of the two phases, this is permitted. Thus, the resulting change in volume is equal to the sum of the volume change of the continuous and the dispersed phase.

$$dV = dV_c + dV_d \quad (11)$$

The volume change of an open system containing the component j can be described by eq. (12) by taking also the change of mass into account. Thus, the volume change can result in a change in pressure at a constant mass and temperature on the one hand or in a change in mass at constant pressure and temperature on the other hand. The factor β describes the isothermal compressibility coefficient of the fluid and γ the isobaric thermic volume expansion coefficient (Ivantysyn and Ivantysynova 2001). The change in mass of the component j arises from the change in the total mass of the systems and the change in the composition of the fluid described by the mass fraction amendment.

$$dV_j = \beta_j V_j dp + \gamma_j V_j dT + \frac{V_j}{m_j} dm_j$$

$$\text{with} \quad dm_j = \mu_j dm + m d\mu_j \quad (12)$$

Equation (12) can be inserted in Equation (11) for each of the two phases with indexes d for the dispersed phase and c for the continuous phase. The void fractions ε_j and the mass fractions μ_j link the two phases, see Equations (13) and (14).

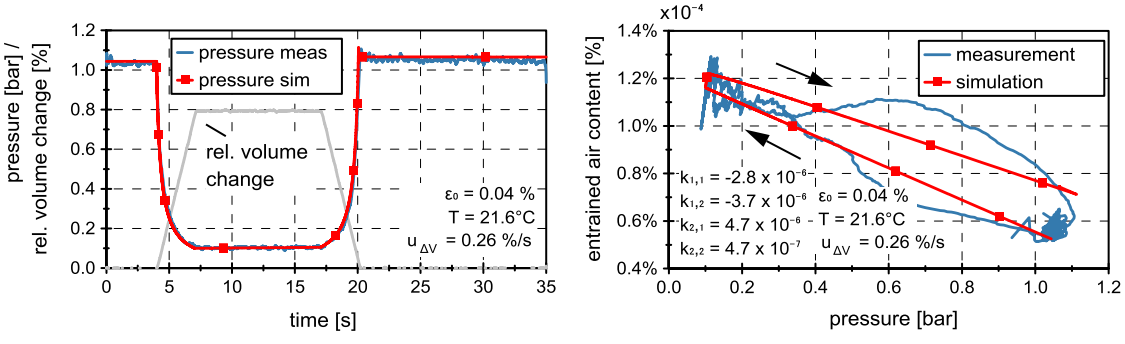

Figure 8. Experimental validation of the proposed mass-transfer model.

$$\varepsilon_d = \frac{V_d}{V_c + V_d} = 1 - \varepsilon_c \tag{13}$$

$$\mu_d = \frac{m_d}{m_c + m_d} = 1 - \mu_c \tag{14}$$

The void fraction and the mass fraction are also directly linked to each other, see Equation (15).

$$\varepsilon_d = \frac{\frac{m_c}{V_c}\mu_d}{\frac{m_d}{V_d}\mu_c + \frac{m_c}{V_c}\mu_d}, \quad \mu_d = \frac{\frac{m_d}{V_d}\varepsilon_d}{\frac{m_d}{V_d}\varepsilon_d + \frac{m_c}{V_c}\varepsilon_c} \tag{15}$$

The pressure change in a two phase system results in Equation (16) by integration Equation (12)–(15) for the two phases in Equation (11), see also Schrank (2015).

$$dp = \frac{1}{\beta_c\varepsilon_c + \beta_d\varepsilon_d}\left(\frac{dm}{m} - \frac{dV}{V} + \left(\frac{\varepsilon_d - \mu_d}{\mu_d\mu_c}\right)d\mu_d + (\gamma_c + \varepsilon_d(\gamma_d - \gamma_c))dT\right) \tag{16}$$

The first factor corresponds to the bulk modulus described above. This new two-phase bulk modulus consists of the pressure-dependent isothermal compression coefficient of the two considered phases and of the actual pressure-dependent void fraction of the dispersed air phase.

$$E_{2ph} = \frac{1}{\beta_c(1 - \varepsilon_d) + \beta_d\varepsilon_d} \tag{17}$$

This description of the effective two-phase bulk modulus differs from the description in Equations (3), (7), and (8). In the isothermal case however, the results are identical when considering that in Equation (3) the void fraction of air has to be calculated at atmospheric pressure.

5. Experimental validation of the model

The model to calculate the pressure and the mass transfer between dissolved and entrained air is finally implemented into Matlab Simulink. The initial conditions for the simulation are taken from the initial conditions of the measurements. In addition, the measured volume change is used for the simulation to calculate the pressure. The parameters needed for the mass transfer model were taken from the simulations shown above fitted with measurements below atmospheric pressure. Figure 9 shows the measured and calculated results above atmospheric pressure. Here, the pressure is plotted over the relative volume change of the sealed chamber. The hysteresis in the pressure build-up and release can clearly be reproduced with the newly established model. The results of measurements and simulations are widely congruent. In addition, the accuracy of the model is also good when different initial air contents are considered, see Figure 10. Here measurements and simulations of the pressure build-up and release are shown for four different initial void fractions.

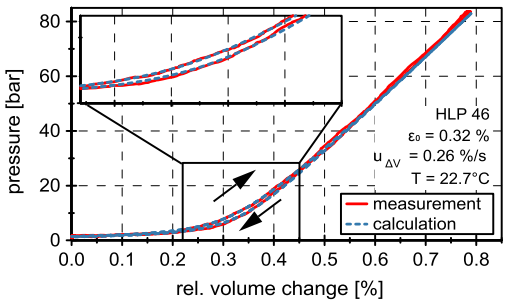

Figure 9. Experimental validation of the proposed pressure calculation model.

All measurements are performed with the same mineral oil HLP46 and the same volume change rate. Therefore the parameters for the mass transfer model are kept constant for all simulations. By comparing the simulation results to the measurements it can be seen that the simulation of the hysteresis due to the absorption and release of air is in good agreement with the measurements.

6. Summary and conclusion

Due to increasing requirements for technical systems and the increasing computing power of modern computers the development of better simulations is required. In particular, an improvement in accuracy combined with an acceptable computational effort of creating these simulation models is important for a time- and cost-effective development and optimization process. For this,

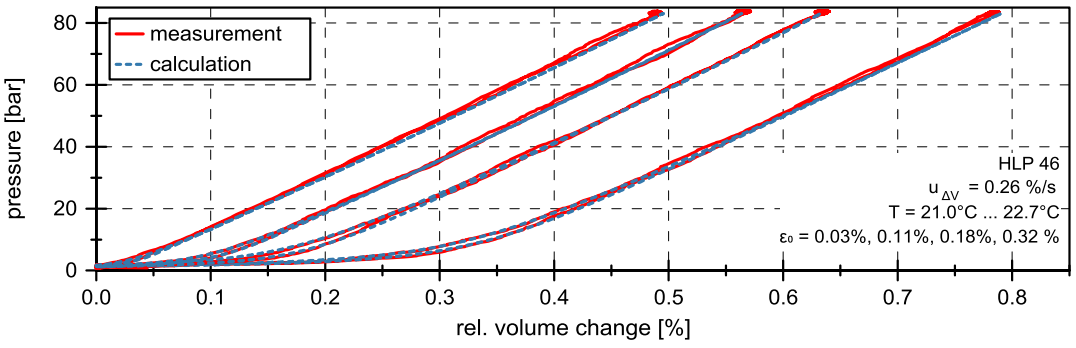

Figure 10. Experimental validation for different void fractions.

the one-dimensional system simulation is an established tool in fluid power. Due to the increasing power density and efficiency of hydraulic systems, impurities and contaminations inside the fluid gain importance as they highly impact the system and its behaviour. Particularly entrained air in hydraulic systems results in a reduction in stiffness and a modified static and dynamic behaviour.

The modelling of this influence of entrained air in hydraulic systems is complex as air can be dissolved into the hydraulic fluid. The amount depends on the static pressure. Therewith, the amount of entrained air inside the fluid changes with a change in pressure. To model the most important parameter in hydraulic systems, the pressure build-up and release, first a mass transfer model between entrained and dissolved air was developed and presented in this paper. This model not only considers the static pressure but also the pressure change velocity as it was found to be an influencing parameter as well. However, it is only a very simple model to calculate the mass transfer between entrained and dissolved air. This physical diffusion process is in reality very complex and depends on much more factors than the pressure and the pressure change rate, e.g. the radius of the individual bubbles, the surface tension, viscosity etc. For a more precise model, these factors have to be investigated and included with the consequence of an enlargement of calculation time.

Finally, the model to calculate the pressure change including the pressure-dependent change in fluids composition was presented and validated by measurements. This model can now be integrated in one-dimensional simulation tools to allow the more accurate prediction of a multi-phase fluid behaviour. Therefore, existing simulation tools that are based on volume conservative calculations must be transferred to a mass conservative calculation basis. An additional advantage of this transfer is also the improving accuracies in high pressure regimes where the pressure dependent change in density is relevant. This will help to improve the accuracy of simulation tools widely used in fluid power.

Notes on contributors

Katharina Schmitz (Nee Schrank) studied Mechanical Engineering at RWTH Aachen University and Carnegie Mellon University from 2005 to 2010. Since September 2010 she is a member of the scientific staff at the Institute for Fluid Power Drives & Controls (IFAS) at RWTH Aachen University.

Hubertus Murrenhoff is director of the Institute for Fluid Power Drives & Controls (IFAS) at RWTH Aachen University. Main research interests cover hydraulics and pneumatics including components, systems, controls, simulation programs and the applications of fluid power in mobile and stationary equipment.

Nomenclature

E	bulk modulus	[bar]
E_0	bulk modulus at atmospheric pressure	[bar]
E_{2ph}	bulk modulus of a two-phase fluid	[bar]
k	Parameter for the mass transfer model	[–]
m	mass	[kg]
$m_{g,d}$	mass of dissolved air	[kg]
$m_{g,e}$	mass of entrained air	[kg]
M	fluid dependent pressure factor for bulk modulus	[–]
n	polytropic exponent	[–]
p	pressure	[bar]
p_0	atmospheric pressure	[bar]
p_c	critical pressure	[bar]
p_s	saturation pressure	[bar]
p_{vap}	vapor pressure	[bar]
T	temperature	[°C]
$u_{\Delta V}$	volume change velocity	[m/s]
V	volume	[m^3]
V_c	volume of the continuous phase	[m^3]
V_d	volume of the disperse phase	[m^3]
β	isothermal compressibility coefficient	[bar^{-1}]
γ	isobaric thermic volume expansion coefficient	[K^{-1}]
ε	void fraction of dispersed phase	[–]
ε_0	void fraction of dispersed phase at atmospheric pressure	[–]
$\varepsilon_{g,e}$	void fraction of entrained air	[–]
μ	mass fraction of free air	[–]
μ	mass fraction of dispersed phase	[–]
$\mu_{g,e}$	mass fraction of entrained air	[–]
μ_{MT}	mass fraction of air being released from oil	[–]
θ	ratio of entrained air and overall air	[–]

Disclosure statement

No potential conflict of interest was reported by the authors.

References

Esqué, S. and Ellman, A. 2005. An efficient numerical method for solving the dynamic equations of complex fluid power systems. *In*: *Proceedings of the 2005 power transmission and motion control workshop*. Hoboken, NJ: Wiley, 179–191, ISBN: 978-0-470-01677-0.

Gholizadeh, H., 2013. *Modeling and experimental evaluation of the effective bulk modulus for a mixture of hydraulic oil and air*. Thesis (PhD). University of Saskatchewan, Saskatoon, Canada.

Gholizadeh, H., Burton, R. and Schoenau, G. 2012. Fluid bulk modulus: comparison of low pressure models. *International journal of fluid power*, 13 (1), 7–16. doi:10.1080/14399776.2012.10781042

von Grabe, C., Reinertz, O., von Dombrowski, R. and Murrenhoff, H. 2014. *System simulation in DSHplus. Encyclopedia of automotive engineering*. Hoboken, NJ, Wiley, ISBN: 978-0-470-97402-5.

Ivantysyn, J. and Ivantysynova, M., 2001. *Hydrostatic pumps and motors, principles, designs, performance, modelling, analysis, control and testing*. New Delhi: Academia Books International. ISBN: 81-85522-16-2.

Kim, S., 2012. *Measurements of effective bulk modulus and its used in CFD simulation*. Thesis (PhD). RWTH Aachen, Aachen, Shaker, ISBN: 978-3-8440-0895-1.

Manhartsgruber, B., 2013. Experimental results on air release and absorption in hydraulic oil. *In*: *Proceedings of the ASME 2013 fluids engineering division summer meeting*.

Paper No. FEDSM2013-16602. Incline Village, Nevada: ASME.

Murrenhoff, H., 2014. *Fundamentals of fluid power*. Aachen: Shaker, ISBN 978-3-8440-2826-3.

LMS, N.N., 2009. *HYD advanced fluid properties technical bulletin no. 117*. Rev 9 November 2009. LMS Engineering Innovations, LMS Imagine. S.A.

Riedel, C., Murrenhoff, H. and Stammen, C. 2010. Physically correct hydraulic system simulation with mass conservative approach. *In*: *Proceedings of the 7th international fluid power conference*. Aachen: Apprimus, ISBN: 978-3-00-031884-9.

Ruan, J. and Burton, R., 2006. Bulk modulus of air content in a hydraulic cylinder. *In*: *Proceedings of the 2006 ASME international mechanical engineering congress and exposition – IMECE*. Paper No. IMECE2006-15854. Chicago, IL: ASME.

Schrank, K., 2015. *Eindimensionale Hydrauliksimulation mehrphasiger Fluide* [One dimensional fluid power simulation for multi-phase fluids]. Thesis (PhD). Shaker, RWTH Aachen, Aachen, ISBN: 978-3-8440-3656-5.

Schrank, K., Murrenhoff, H. and Stammen, C., 2013. Measurements of air absorption and air release characteristics in hydraulic oils at low pressure. *In*: *Proceedings of the ASME/Bath 2013 symposium on fluid power & motion control*. Paper No. FPMC2013-4450. Sarasota, FL: ASME.

Vacca, A., Klop, R. and Ivantysynova, M., 2010. A numerical approach for the evaluation of the effects of air release and vapour cavitation on effective flow rate of axial piston machines. *International journal of fluid power*, 11 (1), 33–45. doi:10.1080/14399776.2010.10780996.

Zhou, J., Vacca, A. and Manhartsgruber, B., 2013. A novel approach for the prediction of dynamic features of air release and absorption in hydraulic oils. *Journal of fluids engineering (ASME)*, 135, 091305-1–091305-8. doi:10.1115/1.4024864.